Numerical Study of Hall Current Effect on MHD Nanofluid with Inclined Plates in the Presence of Brownian motion and Thermophoresis

[1]G. Gangadhar,[2]K. Sharath Babu,[3]V. Srinivasa Kumar

[1]Department of Mathematics, Malla Reddy Engineering College(Autonomous), Secunderabad, Telangana. India. E Mail: gangadharg001@gmail.com

[2]Department of Mathematics, Matrusri Engineering College,Hyderabad, Telangana,India. E Mail: sharathsiddipet@gmail.com

[3]Department of Mathematics,JNTUH College of Engineering, Kukatpally, Hyderabad, Telangana, India. E Mail: vajhasrinu@gmail.com

[*]Corresponding Author: gangadharg001@gmail.com

Article Info

Page Number: 8261 - 8283

Publication Issue:

Vol 71 No. 4 (2022)

Article History

Article Received*: 25 March 2022*

Revised*: 30 April 2022*

Accepted*: 16 December 2022*

Publication*: 31December 2022*

Abstract

This research article deals with the impact of Hall current on an electrically conducting nanofluid flow past a continuously stretching surface with heat generation/absorption has been explored. Transverse magnetic field with the assumption of small Reynolds number is implemented vertically. Appropriate similarity transformations are utilized to transform the governing partial differential equations into the non-linear ordinary differential equations. Numerical solutions for the dimensionless velocity, temperature and nanoparticle concentration are computed with the help of the shooting method. The impact of each of the Hall current parameter, Brownian motion parameter, Prandtl number, thermophoresis parameter and magnetic parameter on velocity, concentration and temperature, is discussed through graphs. The skin friction coefficient along the x− and z− directions, the local Nusselt number and the Sherwood number are calculated numerically to look into the inside behavior of the emerging parameters.

Keywords: Hall current, MHD, Heat generation, Brownian motion, Thermophoresis

1. Introduction

The use of magnetic field of high intensity to an ionic liquid having less density, the conduction normal to the magnetic field is converted to curling of atomic particles and ions related to magnetic lines of force before occurring the clashing and a current induced perpendicular to both the electric and magnetic fields, is known as Hall effect. This effect is considered with heat or mass transfer analysis under the situation where the effect of the electromagnetic force is strong. Hall current is most prominent on the absolute value and orientation of the current density and thereby on the magnetic force term. Under the effects of Hall currents the convective flow problem with magnetic field is significant in view of engineering uses in electric transformers, transmission lines, refrigeration coils, power generators, MHD accelerators, nanotechnological processing, nuclear energy systems exploiting fluid metals, blood flow control and heating elements. In case of magnetic field of high strength and less density of the gas, the investigation of magnetohydrodynamic flows with Hall current have the best utilizations in the study of Hall accelerators and flight magnetohydrodynamic. Peristaltic flows have vast applications under the effects of applied magnetic field in the magnetohydrodynamic feature of blood, process of dialysis, oxygenation and hypothermia. Exploration of non-Newtonian fluid flows has been the focus of many scientists due to its vast applications in industries and engineering. Important applications are exist in food engineering, petroleum production, power engineering, in polymer solutions and in melt in the plastic processing industries. Hall effect plays an important role when the Hall parameter is high. Hall parameter is the ratio of electron cyclotron frequency to atom-electron collision frequency. So the Hall current effect is high when the electron-atom collision frequency is low [1]. Steady MHD boundary layer flow with free convection over a porous inclined plate was explored by Alam et al. [2] with variable suction and Soret effect in the existence of Hall current. Eldahab [3] studied the free convective MHD flow along with the Hall effects through a stretching sheet. Thamizsudar [4] discussed the impact of Hall current and rotationon the heat and mass transfer of MHD fluid flowing over an exponentially accelerated vertical plate. Ibrahim and Anbessa [5] investigated the mixed convection flow of nanofluid with Hall and ion-slip effects using spectral relaxation method.Raghunath and Mohanaramana [6] studied Hall, Soret, and rotational effects on unsteady MHD rotating flow of a second-grade fluid through a porous medium in the presence of chemical reaction and aligned magnetic field. The chemically reactive second grade via porous saturated space was investigated by Raghunath et al. [7] using a perturbation technique. Veerakrishna et al. [8] have studied Heat and Mass transfer on Free Convective flow of a

Micro-polar fluid through a Porous surface with Inclined Magnetic Field and Hall effects. VeeraKrishna and Chamkha [9] have investigated Hall effects on unsteady MHD flow of second grade fluid through porous medium with ramped wall temperature and ramped surface concentration.

The idea of nanofluid was first introduced by Choi [10] in 1995. The homogeneous mixture of very small particles of size 10−9m and base fluid is called nanofluid. Usually Al, Cu, Ag, T iO_2, $Al2O_3$ etc are used as nanoparticles with base fluids like oil, ethylene glycol, water, etc. While using the nanofluids, the maximum possible thermal properties are targeted to achieve with the least feasible concentration by systematic dispersion and substantial suspension of nanoparticles in the base fluids [11, 12]. These fluids are fit for enhancing the thermophysical properties, for example, thermal diffusivity, convective heat transfer coefficient, viscosity, and thermal conductivity when compared with those of the base liquids like ethylene, tri-ethylene glucose, water or other coolants, polymer solutions and biofluids as expatiated by Choi [13] and Wong and Leon [14]. These fluids possess the distinguished physical and chemical properties and can easily pass through the microchannels and capillaries and don't block the flow. Fuel cells, hybrid-powered instruments, automotive, food handling industry and refrigeration are few pertinent examples of nanofluids. Buongiorno [15] considered the Brownian diffusion and thermophoresis slip mechanism for the relative velocity of the base fluid and nanoparticles.

Magnetic nanofluids is another imperative subbranch of nanofluids as it has momentous contribution in number of industrial and engineering fields [16]. Hydrodynamic characteristics and heat transfer rate is further manipulated when the magnetic field is applied across the flow of nanofluids. Often aluminum oxide and magnetite are oppressed during the formulation of such fluids. Sheikholeslami et al. [17] investigated the force convection heat transfer of magnetic nanofluids flow in a lid driven semi-annulus enclosure. They used the two phase model for the simulation of nanofluids. They concluded that higher values of Lewis and Hartmann number decrease the rate of heat flux, but it is augmented for the larger values of Reynolds number. Abbasi et al. [18] considered the boundary layer flow of two dimensional Jeffrey nanofluid with hydromagnetic effects over a linearly stretched sheet.

The process of irregular heat generation or absorption has widespread significances in biomedical and many engineering activities such as radial diffusers, the intention of thrust bearing, and crude oil recovery. Polymer processing, space technology, production of glass and heating a room by the open hearth fireplace are some useful industrial and engineering application of

radiation. Abel and Nandeppanavar [19] have investigated the impact of variable heat absorption/generation on magnetohydrodynamic flow of non-Newtonian liquid across a stretching surface. It was reported that the local Nusselt number is reduced when the irregular heat source/sink parameters are increased. Sandeep and Sulochana [20], Sandeep [21], Kumar et al. [22], and Ramadevi et al. [23] examined the combined influence of thermal and mass transfer features of non-Newtonian liquids due to stretching of a surface. A numerical treatment was presented with the aid of fourth order Runge-Kutta method (RKF-4). It is also noted that the heat sink/source parameters control the mass and thermal performances. Mahanthesh et al. [24] investigated the heat and mass transfer attributes on MHD viscoelastic fluid flow across a stretching surface with thermophoresis and Brownian motion. The impacts of nonlinear radiation, Brownian motion, and quartic chemical reaction on MHD bioconvective flow of nanofluid over an upper horizontal surface of paraboloid revolution was investigated by Makinde and Animasaun [25], who was reported that the Brownian motion increases concentration bulk fluid while thermophoresis declines it.

Thermophoresis is a process in which the fluid particles move towards a cooler region from the warmer [26]. This movement occurs because molecules from the warmer region having high kinetic energy impinge with the molecules having low energy in the cooler region. The velocity gained by the particles is thermophoresis velocity and the force experienced by the particles is called the thermophoresisforce [27]. Particles deposition due to thermophoresis was measured accurately by Tsai et al. [28]. Applications of thermophoresis can be seen in aerosol technology, radioactive particle expulsion in the nuclear reactor safety simulation, heat exchanger corrosion and deposition of silicon thin film. Layers of glass (SiO_2 and GeO_2) are built up by the deposition of particles on the tube wall with the help of modified chemical vapour deposition process. For very small sized chips, the potential failures increase due to the micro contamination by the particle deposition. The process of thermophoresis can be used to inhibit the deposition of small particles on the electronic chips for the purpose of efficiency. The thermophoresis transport of particles in one-dimensional flow for the thermophoresis velocity was studied first time by Goldsmith and May [29]. A theoretical analysis of thermophoresis of aerosol particles in the laminar flow over a horizontal flat plate was presented by Goren [30].

Motivated by the above studies and applications, the present work examines the effect of Hall Current on MHD heat and mass transfer Nanofluid flow with inclined plates in the presence of Brownian motion and Thermophoresis. The effects of flow regulating parameters on the

distributions of flow are presented in tabular and graphical form. This consideration has an important value in engineering and biological research. Analytical and numerical approaches are applied to examine the modeled problem and also compared each other, and good results were obtained.

2. Formulation of the Problem

Here, steady heat andmass transfer ofan incompressible hydromagnetic nanofluid flow along a vertical stretching sheet coinciding with the plane y = 0, has been considered in the presence of the Hall current effects. By keeping theorigin fixed, two opposite and equal forces are assumed to employ along the x-axis so that the sheet stretches linearly in both positive and negative direction (see Figure 1). With the assumption that the Newtonian nanofluid be electrically conducting and heat generating/absorbing, a strong magnetic field has been imposed normal to the direction of flow. Moreover, no electric field has been assumed to apply and the frequency of atom-electron collision has also been considered high for the generation of Hall current effect [31]. Due to the strong magnetic flux density B_0, the Hall current effect is taken into consideration, however the small magnetic Reynolds number is employed and the induced magnetic field is ignored. Hall current effect is strong enough to give rise to a force in the z−direction and a cross flow is induced in the same direction which causes a three dimensional flow. It is further assumed that there are no variations in the flow, heat and mass transfer in the z-direction. This assumption can be achieved by taking the sheet of infinite width. Non-conducting plate is considered so that the generalized Ohm's law [32] gives J_y=0 in the flow field. Brownian motion and thermophoresis effects are considered using the Buongiorno model [33] for the nanofluid. Further, the effects of viscous dissipation and Joule heating are ignored.

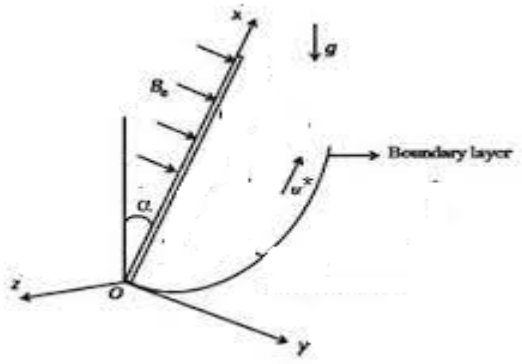

Figure: 1. Physical configuration

By the above mentioned assumptions and Boussinesq approximation, the mathematical form of the problem is

$$\frac{\partial u}{\partial x}+\frac{\partial u}{\partial y}=0 \tag{1}$$

$$u\frac{\partial u}{\partial x}+v\frac{\partial u}{\partial y}=\nu\frac{\partial^2 u}{\partial y^2}-\frac{\sigma B_0^2}{\rho\left(1+m^2\right)}\left(mw+u\right)+ g_C\beta_T(T-T_\infty)\,Cos\alpha+g_C\beta_C(C-C_\infty)\,Cos\alpha \tag{2}$$

$$u\frac{\partial w}{\partial x}+v\frac{\partial w}{\partial y}=\nu\frac{\partial^2 w}{\partial y^2}+\frac{\sigma B_0^2}{\rho\left(1+m^2\right)}\left(mu-w\right) \tag{3}$$

$$u\frac{\partial T}{\partial x}+v\frac{\partial T}{\partial y}=\frac{k}{\rho C_p}\frac{\partial^2 T}{\partial y^2}+\frac{1}{\rho C_p}\left(\frac{ka}{\nu}\right)\left[A^*(T_w-T_\infty)e^{-\eta}+B^*(T-T_\infty)\right] +\tau\left(D_B\frac{\partial C}{\partial y}\frac{\partial T}{\partial y}+\frac{D_T}{T_\infty}\left(\frac{\partial T}{\partial y}\right)^2\right) \tag{4}$$

$$u\frac{\partial C}{\partial x}+v\frac{\partial C}{\partial y}=D_B\frac{\partial^2 C}{\partial y^2}+\frac{D_T}{T_\infty}\frac{\partial^2 T}{\partial y^2} \tag{5}$$

When both A* and B* are positive, we have the heat generation case whereas for the negative values of both of them, there is the internal heat absorption.

The corresponding boundary conditions for the governing PDEs are

$$\begin{aligned} &u=ax,\quad v=0,\quad w=0,\quad T=T_w,\quad C=C_w && \text{at } y=0\\ &u\to 0,\quad v\to 0,\quad w\to 0,\quad T\to T_\infty \quad C\to C_\infty && \text{as } y\to\infty \end{aligned} \tag{6}$$

The similarity transformation used to transform the PDEs to dimensionless ODEs

$$\eta=\sqrt{\frac{a}{\nu}}y,\ \psi(x,y)=\sqrt{a\nu}\,x\,f(\eta),\ w=ax\,g(\eta)\ \phi(\eta)=\frac{C-C_\infty}{C_w-C_\infty},\ \theta(\eta)=\frac{T-T_\infty}{T_w-T_\infty}\ \theta=\frac{T}{T_w} \tag{7}$$

Substitute Eq. (7) into Eq. (2), (3), (4), (5) and Eq. (6) yields to obtain the subsequent non dimensional equations

$$f'''+ff''-f'^2+Gr_x\theta Cos\alpha+Gr_c\phi Cos\alpha-\frac{M}{1+m^2}\left(f'+mg\right)=0 \tag{8}$$

$$g''+fg'-f'g+\frac{M}{1+m^2}\left(mf'-g\right)=0 \tag{9}$$

$$\theta'' + \Pr\ f\theta' + \Pr N_b\left(\theta'\phi' + \frac{N_T}{N_b}\theta'^2\right) + A^* e^{-\eta} + B^*\theta = 0 \tag{10}$$

$$\phi'' + \Pr\ L_e\ f\ \phi' + \frac{N_t}{N_b}\theta'' = 0 \tag{11}$$

The correlated Dimensionless boundary conditions (BCs) are

$$\begin{aligned} &f(0)=0,\quad f'(0)=1,\quad g(0)=0,\quad \theta(0)=0,\quad \phi(0)=1 \qquad at \quad \eta=0 \\ &f'(\eta)\to 0,\quad g(\eta)\to 0,\quad \theta(\eta)\to 0,\quad \phi(\eta)\to 0 \qquad as \quad \eta\to\infty \end{aligned} \tag{12}$$

In the equations that do not include dimensions, the important parameters are defined as

$$\begin{aligned} &M=\frac{\sigma B_0^2}{\rho a},\quad \Pr=\frac{\nu}{\alpha}=\frac{\nu\rho C_p}{k},\quad L_e=\frac{\alpha}{D_B},\quad Gr_x=\frac{g_c\beta_T(T_w-T_\infty)}{a^2 x}, \\ &N_b=\frac{\tau D_B(C_w-C_\infty)}{\nu},\quad N_t=\frac{\tau D_T(T_w-T_\infty)}{\nu},\ Gr_C=\frac{g_c\beta_C(C_w-C_\infty)}{a^2 x} \end{aligned} \tag{13}$$

3. Physical quantities of Interests

The local skin friction coefficient in the direction of x Cf_x, and in the direction of z Cf_z, the local Nusselt number Nu_x, and the local Sherwood number Sh_x are the physical quantities of relevance that influence the flow. These numbers have the following definitions:

$$C f_x=\frac{2\tau_{wx}}{\rho(ax)^2},\ Cf_z=\frac{2\tau_{wz}}{\rho(ax)^2},\ Nu_x=\frac{xq_w}{k(T_w-T_\infty)},\ Sh_x=\frac{x\,j_w}{D_B(C_w-C_\infty)} \tag{14}$$

where τwx, τwy, qw and jw are the wall skin friction, wall heat flux and wall mass flux respectively given by

$$\tau_{wx}=\mu\left[\frac{\partial u}{\partial y}\right]_{y=0},\quad \tau_{wz}=\mu\left[\frac{\partial w}{\partial y}\right]_{y=0},\ q_w=-k\left[\frac{\partial T}{\partial y}\right]_{y=0},\quad j_w=-D_B\left[\frac{\partial C}{\partial y}\right]_{y=0} \tag{15}$$

The coefficient of skin friction, the Nusselt number, and the Sherwood number are all expressed in their non-dimensional versions in terms of the similarity variable as follows:

$$\mathrm{Re}_x^{1/2} Cf_x = 2f''(0),\quad \mathrm{Re}_x^{1/2} Cf_z = 2g'(0),\ \mathrm{Re}_x^{1/2} Nu_x = -\theta'(0),\ \mathrm{Re}_x^{1/2} Sh_x = -\phi'(0) \tag{16}$$

4. Solution methodology

The system of non-linear ODEs (8-11) subject to the boundary conditions 12 has been solved by the shooting method for various values of the involved parameters. We observed through graphs that for η > 8, there is no significant variation in the behavior of solutions. Therefore, on the basis

of such computational experiments, we are pondering [0, 8] as the domain of the problem instead of [0, ∞). We denote f by y_1, g by y_4, θ by y_6 and φ by y_8 for converting the boundary value problem (4.9-4.13) to the following initial value problem consisting of 9 first order differential equations.

$$y_1' = y_2,$$

$$y_2' = y_3,$$

$$y_3' = -y_1 y_3 + y_2^2 - Gr_x y_6 + Gr_c y_8 + \frac{M}{1+m^2}(y_2 + m y_4),$$

$$y_4' = y_5,$$

$$y_5' = y_2 y_4 - y_1 y_5 - Gr_x y_6 + Gr_c y_8 - \frac{M}{1+m^2}(-y_4 + m y_2),$$

$$y_6' = y_7,$$

$$y_7' = -\Pr y_1 y_7 - \Pr N_b \left(y_9 y_7 + \frac{N_T}{N_b} {y_7}^2 \right) - A^* e^{-\eta} - B^* y_6,$$

$$y_8' = y_9,$$

$$y_6' = -\Pr\ L_e\, y_1\, y_9 - \frac{N_t}{N_b} y_7'$$

5. Results and Discussions

To envision the effect of various physical parameters on tangential velocity $f^i(\eta)$, transverse velocity g(η), nanoparticle concentration φ(η) and temperature θ(η) profiles, Figures 4.2-4.26 are plotted. In all these computations, unless mentioned, otherwise we have considered Nb= 0.3, α=π/3, Nt= 0.7, P r= 0.71, Le = 0.6, M= 0.5, m= 0.2, Grx = 0.5, Gr = 0.5, A^*=0.01, B^*= 0.01

Figures 2 to 5 shows the effect of magnetic parameter M on the tangential velocity f ’(η), transverse velocity g(η), temperature θ(η), and concentration φ(η) profiles, respectively. The velocity profile f’(η) decreases with an increase in the values of M, the same behavior has observed transverse velocity g(η), and temperature θ(η) and concentration φ(η) profiles increase as M increases. As M increases, a drag force, called Lorentz force increases. Since this force opposes the flow of nanofluid, velocity in the flow direction decreases. Moreover, since an electrically conducting nanofluid with the strong magnetic field in the direction orthogonal to the flow are considered, an increase in M increases the force in the z-direction which results in an diminishes in the transverse velocity profile g(η).

In Figures 6-13 the effects of the thermal Grashof Grx and concentration Grashof Grc numbers on the tangential velocity $f''(\eta)$, the transverse velocity $g(\eta)$, temperature and concentration are displayed respectively. As the Grashof number is a ratio of the buoyancy force to the viscous force and it appears due to the natural convection flow, so an increase in the tangential velocity as well as the lateral velocity of the fluid is observed when the thermal and the concentration Grashof numbers are increased as shown in figures 6,7,10,11. It happens because of the fact that higher the Grashof number implies higher the buoyancy force which means higher the movement of the flow. Figures 8 and 9 depict the influence of the solutal Grashof number on the temperature and the concentration profile respectively. An increase in the solutal Grashof number means a decrease in the viscous force which reduces the temperature and the concentration of the fluid. Similarly temperature is reduced when the thermal Grashof number is enhanced and this phenomenon can be observed in Figures 12-13.

Figures 14-17 illustrate the impacts of the Hall parameter m on tangential velocity $f'(\eta)$, transverse velocity $g(\eta)$, nanoparticle concentration $\varphi(\eta)$ and temperature $\theta(\eta)$ profiles, respectively. It is observed that both the velocity $f'(\eta)$ and $g(\eta)$ profiles increase as m increases. But, the temperature and concentration profiles decrease with an increase in m as shown in Figs. 16 and 17. This is because the enclosure of Hall parameter decreases the resistive force caused by the magnetic field due to its effect of reducing the effective conductivity. Hence, the velocity component increases as the Hall parameter increases.

Influence of Brownian motion parameter Nb on the temperature and concentration profiles is studied in Figures 18 and 19. From these figures, we notice that an enhancement in the values of Nb gives rise to the temperature, while it causes a decrease in the nanoparticle concentration profile. Brownian motion is the random motion of nanoparticles suspended in the fluid, caused by the collision of nanoparticles with the fluid particles. An increment in the thermophoretic effect causes an increment in the Brownian motion effect which results in the rise of the temperature due to the increment in the kinetic energy.

Figures 20 and 21 illustrate the effect of thermophoresis parameter Nt on the temperature and the nanoparticles concentration profile. One can observe that temperature and concentration fields increase with an enhancement in Nt. Thermophoresis parameter plays an important role in the heat transfer flow. Thermophoresis force enhances when Nt is increased which tends to move the nanoparticles from the hot region to the cold and as a result the temperature and the boundary layer thickness increase.

Figures 22 and 23 shows the impact of the Lewis number Le on temperature and nanoparticle concentration profiles respectively. It is observed that the temperature increases by increasing Le while concentration decreases with an increase in the Lewis number.

Figures 24-27 illustrate the impacts of the Inclined parameter α on tangential velocity $f^{i}(\eta)$, transverse velocity g(η), nanoparticle concentration φ(η) and temperature θ(η) profiles, respectively. It is observed that both the velocity f'(η), g(η), temperature and concentration profiles decrease with an increase in α.

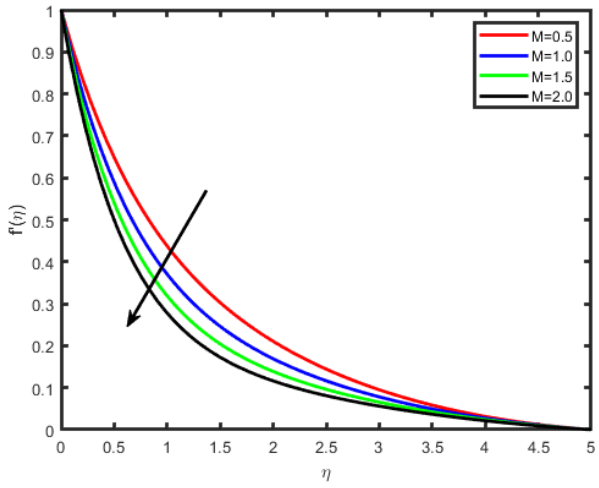

Figure: 2. Effect of M on f'(n)

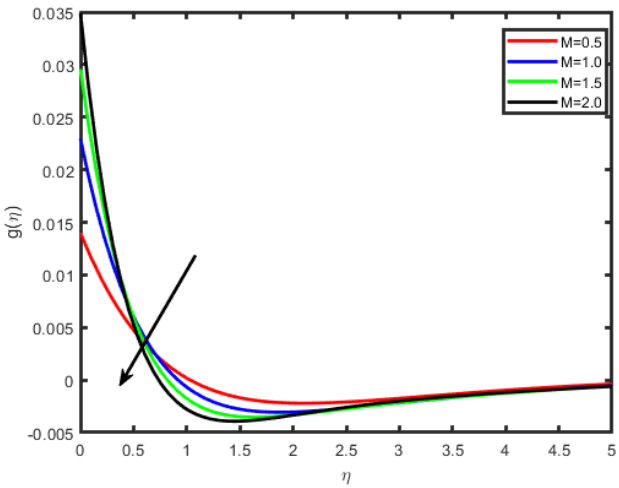

Figure: 3. Effect of M on g(n)

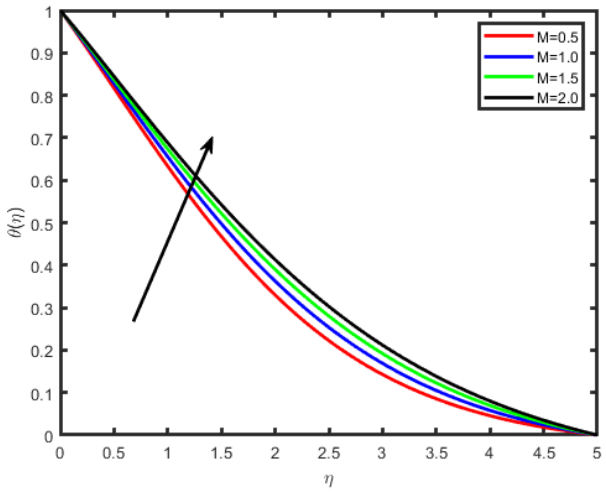

Figure: 4. Effect of M on θ(n)

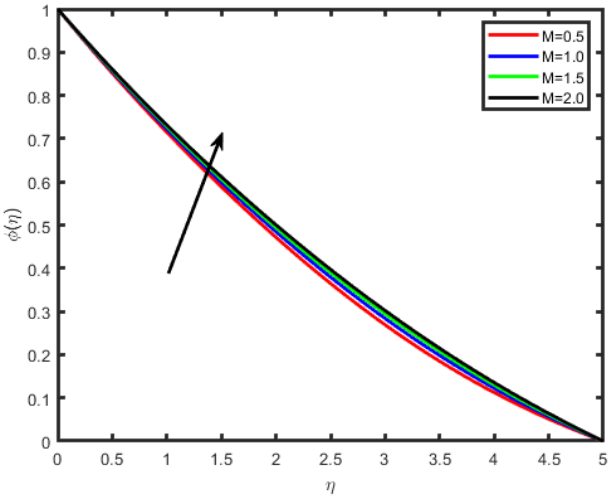

Figure: 5. Effect of M on ϕ (n)

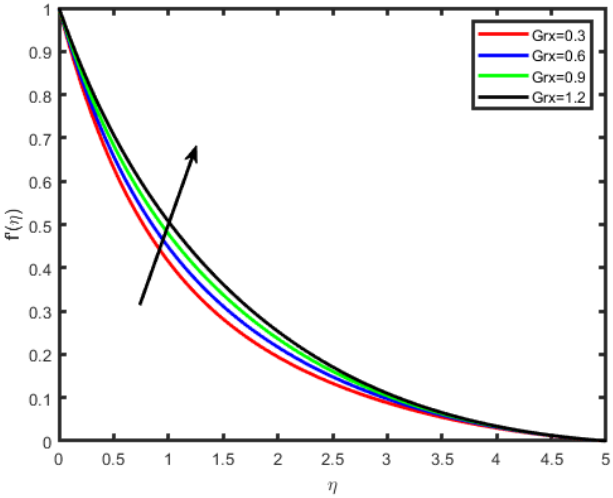

Figure: 6. Effect of Grx on f ̒(n)

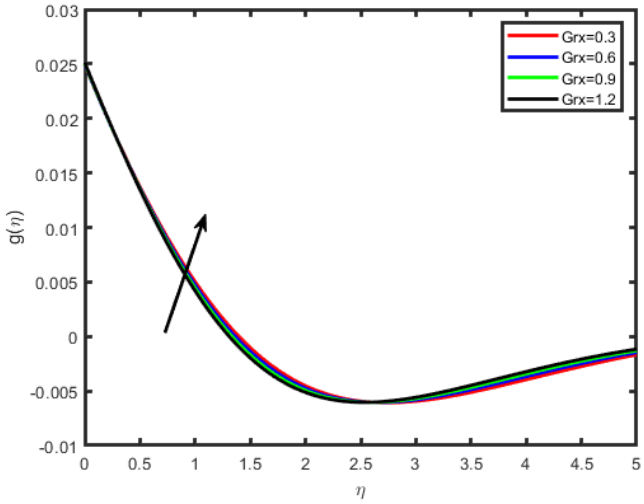

Figure: 7. Effect of Grx on g (n)

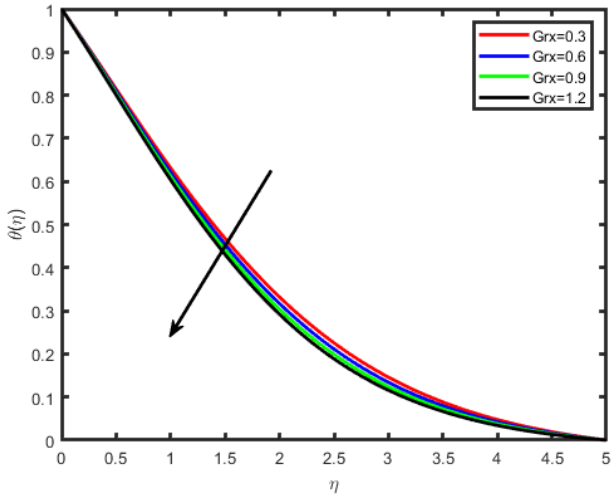

Figure: 8. Effect of Grx on θ (n)

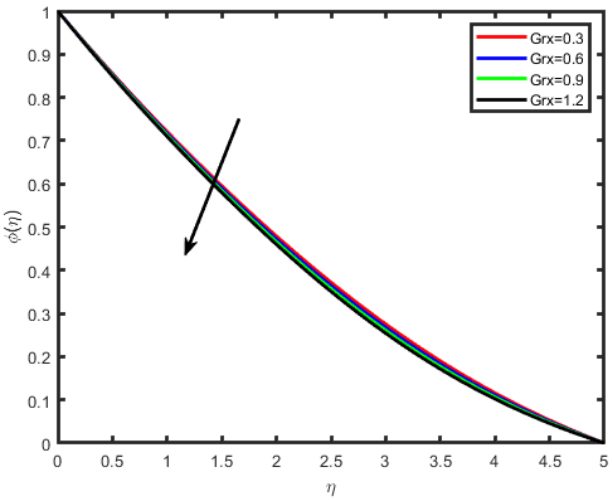

Figure: 9. Effect of Grx on ϕ (n)

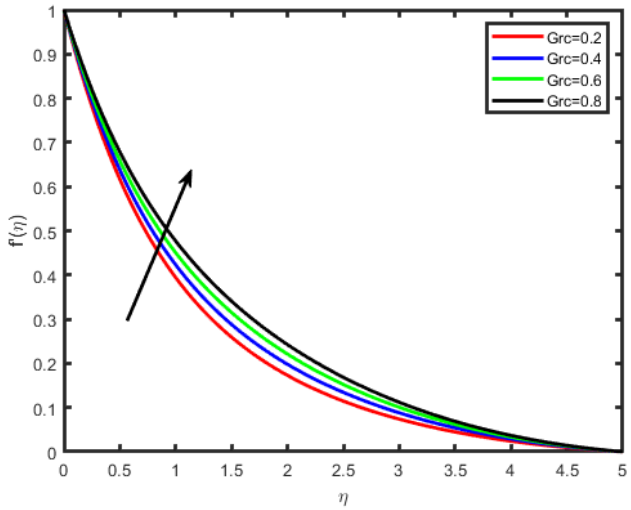

Figure: 10. Effect of Grc on f (n)

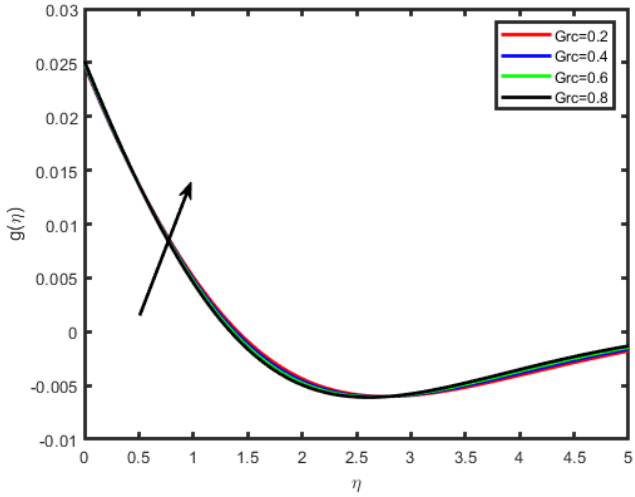

Figure: 11. Effect of Grc on g (n)

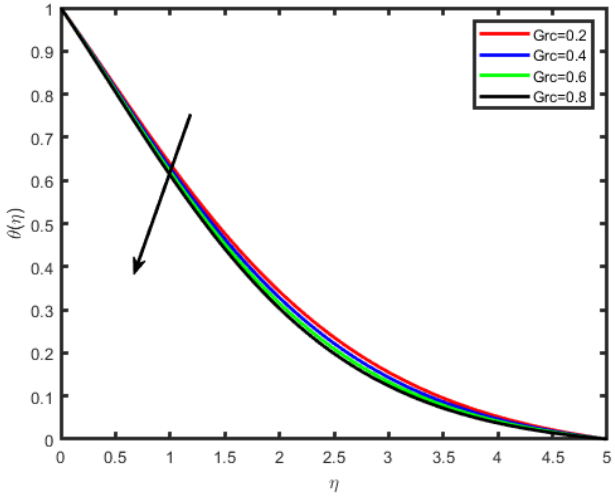

Figure: 12. Effect of Grc on θ (n)

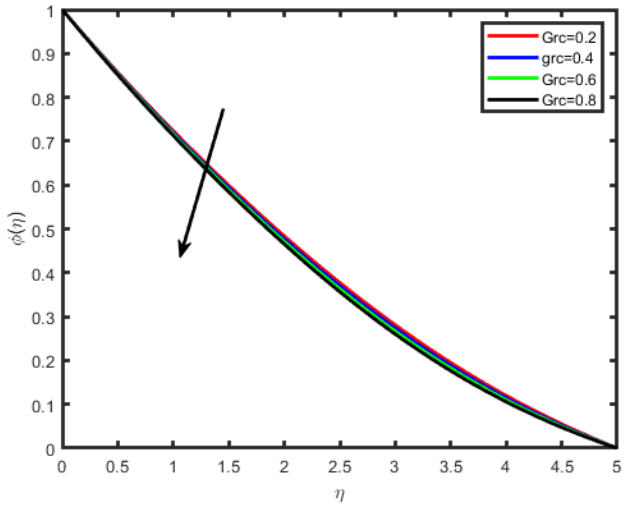

Figure: 13. Effect of Grx on ϕ (n)

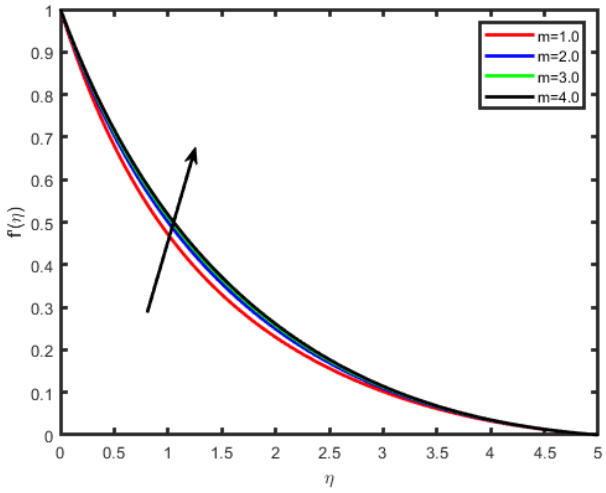

Figure: 14. Effect of m on f ̀(n)

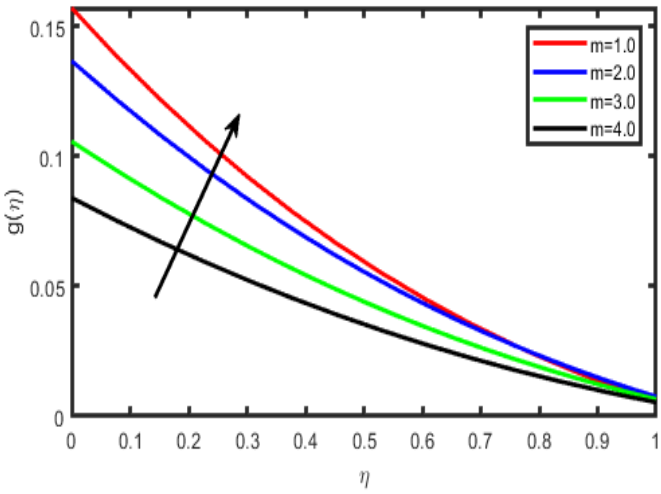

Figure: 15. Effect of m on g(n)

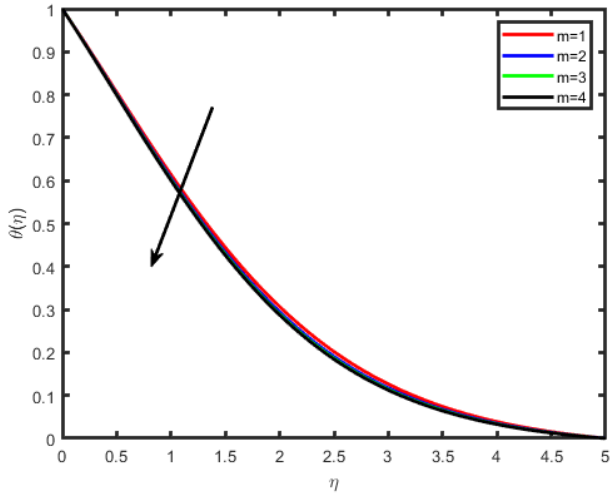

Figure: 16. Effect of m on θ(n)

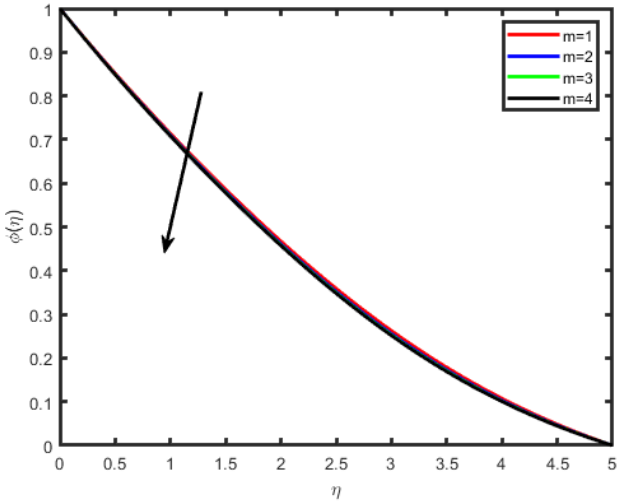

Figure: 17. Effect of m on ϕ(n)

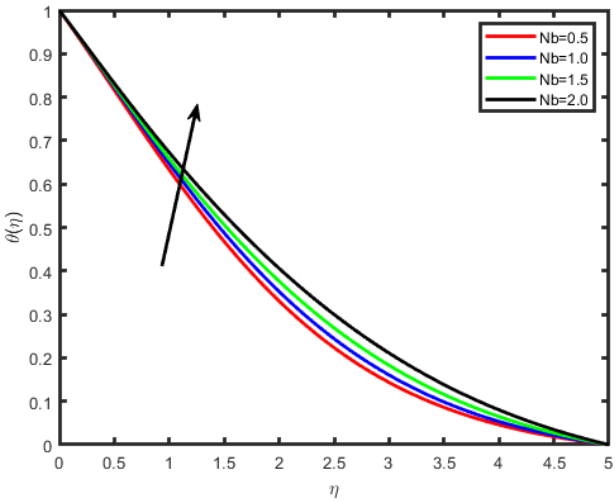

Figure: 18. Effect of Nb on θ(n)

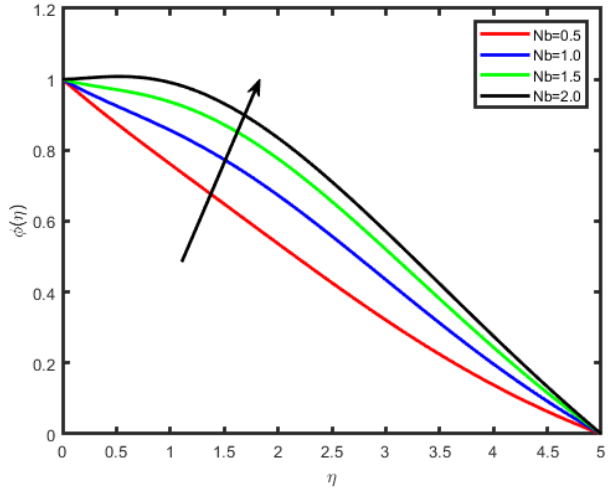

Figure: 19. Effect of Nb on ϕ(n)

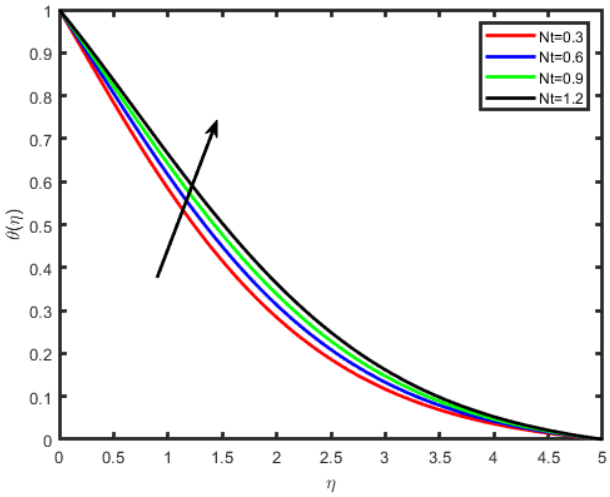

Figure: 20. Effect of Nt on θ(n)

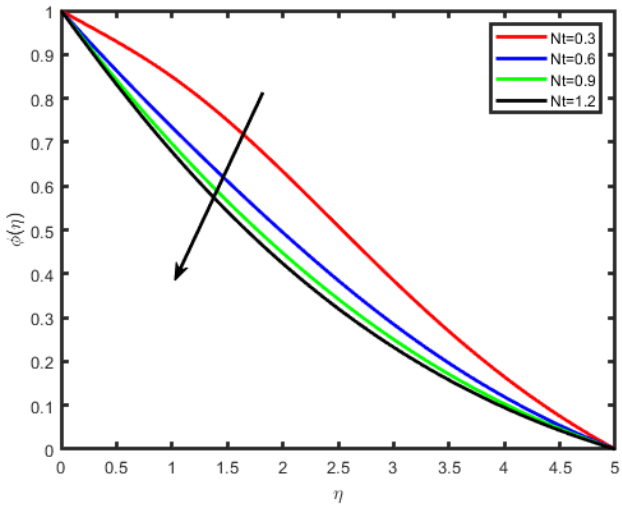

Figure: 21. Effect of Nb on ϕ(n)

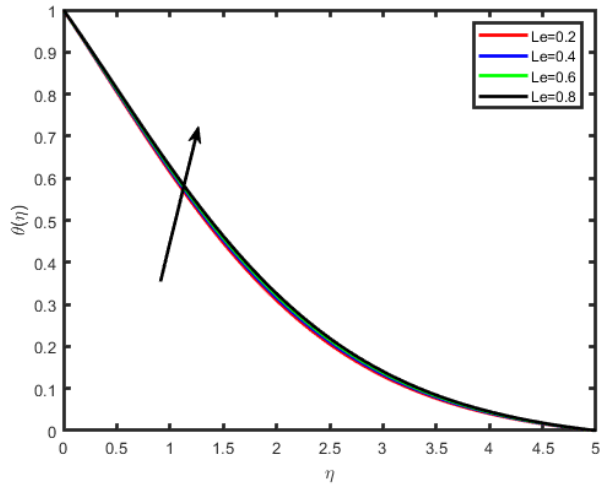

Figure: 22. Effect of Le on θ(n)

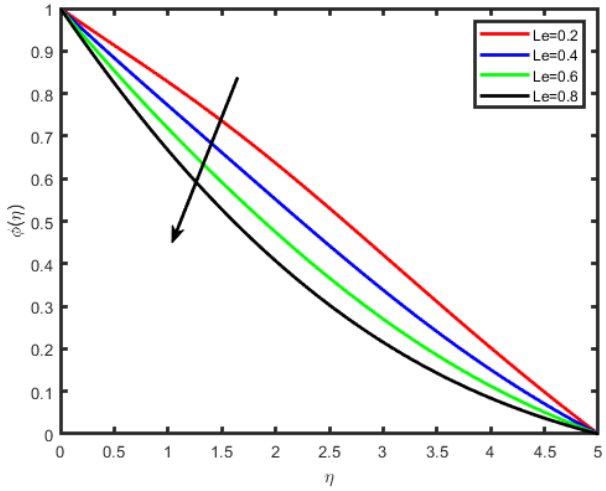

Figure: 23. Effect of Le on ϕ(n)

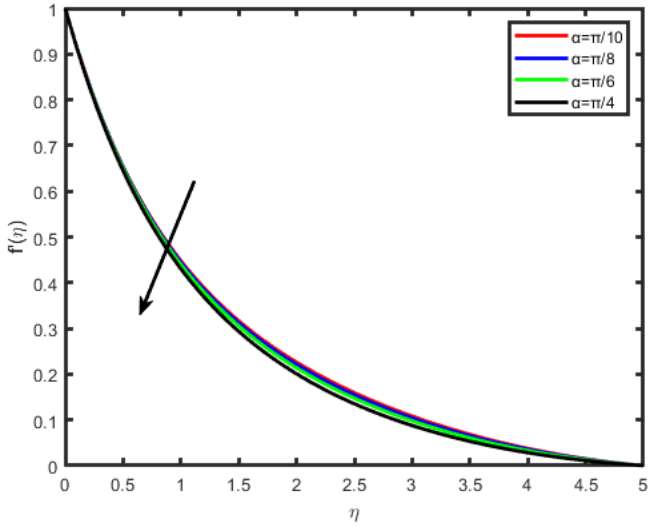

Figure: 24. Effect of α on $f^{'}$(n)

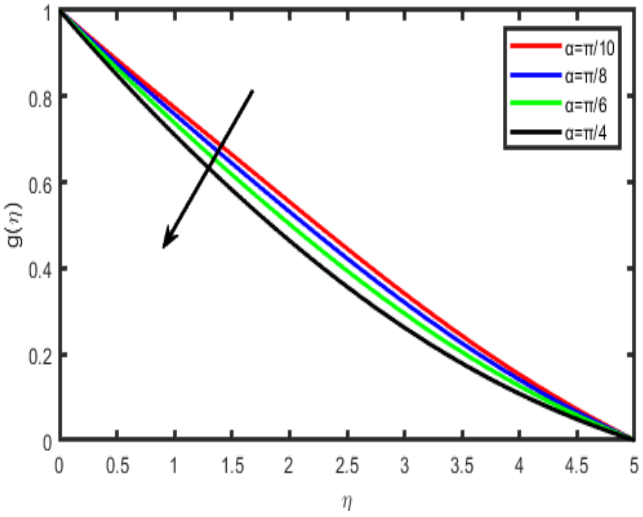

Figure: 25. Effect of α on g(n)

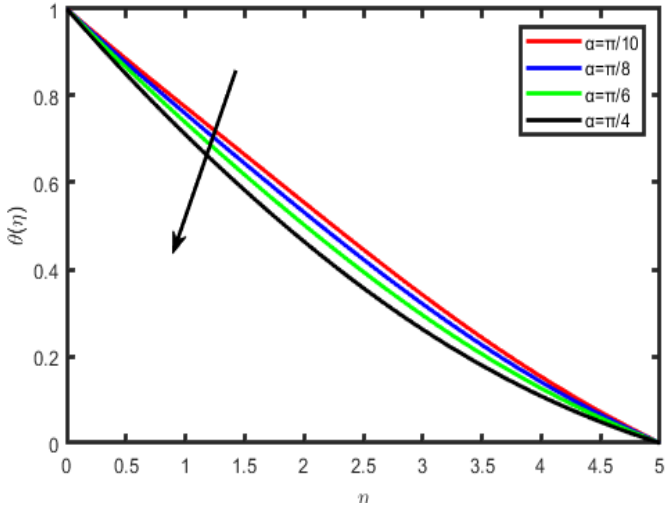

Figure: 26. Effect of α on θ(n)

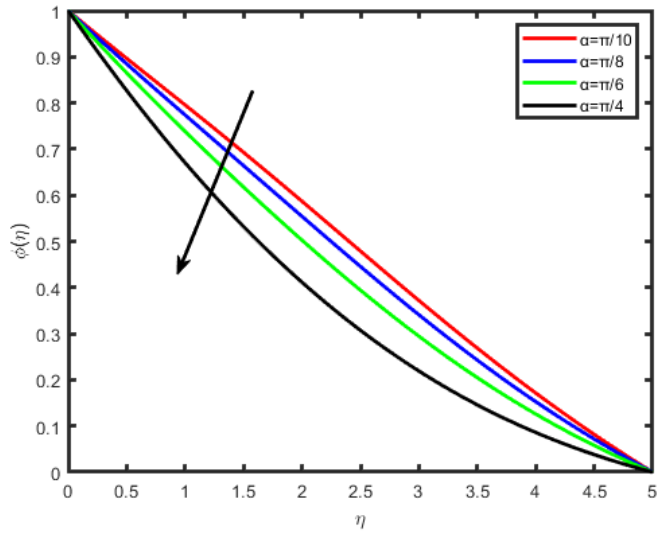

Figure: 27. Effect of α on ϕ(n)

The impact of the various physical parameters on the local Sherwood number, skinfriction coefficient and local Nusselt number, mathematical results are achieved for Nb= 0.3, α=π/3, Nt= 0.7, P r= 0.71, Le = 0.6, M= 0.5, m= 0.2, Grx = 0.5, Gr = 0.5, A^*=0.01, B^*= 0.01, and are enumerated as shown in Table 1. it is viewed that the skin-friction coefficient in x− direction decreases with an increase in the thermal Grashof number Grx, the mass Grashoff number Grc, Hall current parameter m, and Brownian motion parameter Nb, while it increases for the increasing value of magnetic parameter M and Prandtl number Pr, and thermophoresis parameter Nt. A completely opposite behavior is recorded for the coefficient of the skin-friction in the z-direction. Nusselt number increases when the Hall current parameter m, thermal Grashof number, the mass Grashoff number, and Prandtl number, increase whereas it is reduced by increasing the value of Magnetic field parameter M. Sherwood number has increasing behavior for thermal Grashof number Grx, Magnetic field parameter M, Brownian motion parameter Nb and thermophoresis parameter Nt, while it has decreasing behavior for Grashoff number Grc and Prandtl number.

For the authentication of the numerical method used, the results were compared with the previously obtained results Ibrahim and Anbessa [5] for various values of parameters and it indicates an excellent accord as shown in Tables 2.

Table1: Numerical values of $\mathrm{Re}_x^{1/2} Cf_x$, $\mathrm{Re}_x^{1/2} Cf_z$, $\mathrm{Re}_x^{1/2} Nu_x$, $\mathrm{Re}_x^{1/2} Sh_x$

Grx	Grc	m	Nb	M	Pr	Nt	-2f''(0)	-2g'(0)	-θ'(0)	-φ'(0)
0.5							1.2547	0.8521	0.5212	0.9514
1.0							0.9978	0.9125	0.5323	0.9912
1.5							0.7354	0.9542	0.5457	1.0245
	0.3						0.9875	0.8512	0.5032	0.1247
	0.6						0.8475	0.9852	0.5124	0.1108
	0.9						0.7125	1.2521	0.5785	0.9178
		1					1.5214	0.8521	0.3145	0.8852
		2					1.0214	0.9547	0.2978	0.7952
		3					0.8125	0.9985	0.2312	0.9452
			0.2				0.9512	0.9521	0.8452	0.5852
			0.4				0.8152	0.9612	0.8215	0.6124
			0.6				0.7125	0.9852	0.8032	0.6978
				0.5			0.9452	1.0254	0.9875	0.7852

				1.0			1.2454	0.9852	0.9125	0.8952
				1.5			1.4035	0.8512	0.8952	0.9452
					0.68		0.9785	1.0214	0.1254	0.9878
					0.71		0.9120	0.9852	0.1578	0.9452
					0.76		0.8452	0.9032	0.1987	0.9231
						0.3	1.5452	0.9852	0.8542	0.5120
						0.6	1.1254	0.9120	0.8125	0.5921
						0.9	0.8752	0.8962	0.7521	0.6120

Table: 2. Comparison of $-\theta'(0)$ for various values of Pr when Nb= 0.3, Nt= 0.7, P r= 0.71, Le = 0.6, M= 0.5, Grx = 0.5, Gr c= 0.5, A^*=0, B^*= 0, m=0, α=0

Pr	Ibrahim and Anbessa [5]	Present values
0.01	0.019887	0.019852
0.72	0.808635	0.807852
1	1.000000	1.000000
3	1.923687	1.924785
10	3.720676	3.732547

6. Conclusion

The influence of the Hall current on the heat and mass transfer of nanofluid flowing across a linearly stretched sheet is the topic that will be discussed in the present paper. The most significant accomplishments have been broken down into the following categories:

i. The temperature increases as the Brownian motion parameter (Nb) values increase, but the concentration profile of nanoparticles decreases.
ii. The temperature and concentration fields intensify with a rise in the Thermophoresis parameter (Nt).
iii. The temperature and concentration profiles tend to fall when the Prandtl number (Pr) is raised.
iv. The temperature increases by increasing Le while concentration decreases with an increase in the Lewis number

v. The velocity increases with enhance of hall parameter (m), where as the reversal behavior has observed in the case of temperature and Concentration.

References

[1] K. Cramer and S. Pai, Magnetofluid dynamics for engineers and applied physicists, McGraw-Hill, New York, vol. 93, 1973.

[2] M. S. Alam, M. Ali, M. A. Alim, and A. Saha, Steady MHD boundary free convective heat and mass transfer flow over an inclined porous plate with variable suction and Soret effect in presence of Hall current, J. Heat Mass Trans., vol. 49, pp. 155–164, 2014.

[3] E. M. Abo-Eldahab, Hall effects on magnetohydrodynamic free convective flow at a stretching surface with a uniform free stream, Phys. Scr., vol. 63, pp. 29–35, 1999.

[4] M. Thamizsudar and J. Pandurangan, Hall effects and rotation effects on MHD flow past an exponentially accelerated vertical plate with combined heat and mass transfer effects, Int. J. Appl. Mech. Engr., vol. 20, pp. 605– 616, 2015.

[5] W. Ibrahim, T. Anbessa, mixed convection flow of nanofluid with Hall and ion-slip effects using spectral relaxation method, Journal of the Egyptian Mathematical Society, 27(52), pp. 1-21, 2019. https://doi.org/10.1186/s42787-019-0042-9

[6] Raghunath K, Mohanaramana R. Hall, Soret, and rotational effects on unsteady MHD rotating flow of a second-grade fluid through a porous medium in the presence of chemical reaction and aligned magnetic field. International Communications in Heat and Mass Transfer, 137, 2022,106287. https://doi.org/10.1016/j.icheatmasstransfer.2022.106287.

[7] Raghunath K, Mohanaramana R, Nagesh G, Charankumar G, Sami Ullah Khan and Ijaz Khan M. Hall and ion slip radiative flow of chemically reactive second grade through porous saturated space via perturbation approach. Waves in Random and Complex Media, 32. doi: 10.1080/17455030.2022.2108555

[8] M. Veerakrishna, P. V. S. Anand, Ali. J. Chamkha, Heat and Mass transfer on Free Convective flow of a Micro-polar fluid through a Porous surface with Inclined Magnetic Field and Hall effects, Volume 10, Issue 3, 2019, pp. 203-223 DO - 10.1615/SpecialTopicsRevPorousMedia.2018026943

[9] M. VeeraKrishna, Ali J. Chamkha. Hall effects on unsteady MHD flow of second grade fluid through porous medium with ramped wall temperature and ramped surface concentration, Physics of Fluids, 30 (2018): 053101.

[10] S. U. S. Choi, "Enhancing thermal conductivity of fluids with nanoparticles, development and applications of non-Newtonian flows," ASME J. Heat Trans., pp. 0–8, 1995.

[11] S. M. S. Murshed, K. C. Leong, and C. Yang, "Thermophysical and electrokinetic properties of nanofluids - a critical review," Appl. Therm. Engr., vol. 28, pp. 2109–2125, 2008.

[12] S. Ozerinc, S. Kakac, and A. Yazicioglu, Enhanced thermal conductivity of nanofluids: a state-of-the-art review, Microfluids Nanofluids, vol. 8, pp. 145–170, 2010.

[13] S. U. S. Choi, Nanofluids: from vision to reality through research, J. Heat Trans., vol. 131, pp. 1–9, 2009.

[14] K. V. Wong and O. Leon, "Applications of nanofluids: current and future," Adv. Mech. Engr., vol. 2010, pp. 1–10, 2010.

[15] J. Buongiorno, "Convective transport in nanofluids applications of nanofluids: current and future," ASME J. Heat Trans., vol. 2010, pp. 240–250, 2006.

[16] S. Das, S. Chakraborty, R. N. Jana, and O. D. Makinde, "Entropy analysis of unsteady magneto-nanofluid flow past accelerating stretching sheet with convective boundary condition," Appl. Math. Mech, vol. 36, pp. 1593–1610, 2015.

[17] M. Sheikholeslami, M. M. Rashidi, and D. D. Ganji, "Numerical investigation of magnetic nanofluid forced convective heat transfer in existence of variable magnetic field using two phase model," J. Mol. Liq., vol. 212, pp. 117–126, 2015.

[18] F. M. Abbasi, S. A. Shehzad, T. Hayat, A. Alsaedi, and M. A. Obid, "Influence of heat and mass flux conditions in hydromagnetic flow of Jeffrey nanofluid," AIP Adv., vol. 5, p. 037111, 2015.

[19] Abel, M.S. and Nandeppanavar, M.M., Heat Transfer in MHD Viscoelastic Boundary Layer Flow over a Stretching Sheet with Non-Uniform Heat Source/Sink, Commun. Nonlin. Sci. Numer. Simul., vol. 14, pp. 2120–2131, 2009.

[20] Sandeep, N. and Sulochana, C., Dual Solutions for Unsteady Mixed Convective Flow of MHD Micropolar Fluid over a Stretching/Shrinking Sheet with Non-Uniform Heat Source/Sink, Eng. Sci. Tech., Int. J., vol. 18, pp. 738–745, 2015.

[21] Sandeep, N., Effect of Aligned Magnetic Field on Liquid Thin Film Flow of Magnetic-Nanofluids Embedded with Graphene Nanoparticles, Adv. Powder Tech., vol. 28, no. 3, pp. 865–875, 2017.

[22] Kumar, K.A., Sugunamma, V., and Sandeep, N., Numerical Exploration of MHD Radiative Micropolar Liquid Flow Driven by Stretching Sheet with Primary Slip: A Comparative Study, J. Non-Equilib. Thermodyn., 2018c. DOI: 10.1515/jnet-2018-0069

[23] Ramadevi, B., Sugunamma, V., Kumar, K.A., and Reddy, J.V.R., MHD Flow of Carreau Fluid over a Variable Thickness Melting Surface Subject to Cattaneo-Christov Heat Flux, Multi. Model. Mater. Struct., vol. 15, no. 1, 2019.

[24] Mahanthesh, B., Gireesha, B.J., and Animasaun, I.L., Exploration of Non-Linear Thermal Radiation and Suspended Nanoparticles Effects on Mixed Convection Boundary Layer Flow of Nanoliquids on a Melting Vertical Surface, J. Nanofluids, vol. 7, pp. 833– 843, 2018.

[25] Makinde, O.D. and Animasaun, I.L., Thermophoresis and Brownian Motion Effects on MHD Bioconvection of Nanofluid with Nonlinear Thermal Radiation and Quartic Chemical Reaction past an Upper Horizontal Surface of a Paraboloid of Revolution, J. Mol. Liq., vol. 221, pp. 733–743, 2016.

[26] W. C. Hinds, "Aerosol technology: properties, behavior, and measurement of airborne particles," John Wiley and Sons, New York, 1982.

[27] A. Y. Bakiera and M. A. Mansour, "Combined magnetic field and thermophoresis particle deposition in free convection boundary layer from a vertical flat plate embedded in a porous medium," Int. J. Thermal. Sci., vol. 11, pp. 65–74, 2007.

[28] C. J. Tsai, J. S. Lin, I. Shankar, G. Aggarwal, and D. R. Chen, "Thermophoretic deposition of particles in laminar and turbulent tube flows," Aerosol Sci. Technol., vol. 38, pp. 131–139, 2004.

[29] P. Goldsmith and F. G. May, "Diffusiophoresis and thermophoresis in water vapour systems, in: Aerosol science," C. N. Davies (Ed.), Academic Press, London,, pp. 163–194, 1966.

[30] S. L. Goren, "Thermophoresis of aerosol particles in laminar boundarylayer on flat plate," J. Colloid Interface Sci., vol. 61, pp. 77–85, 1977.

[31] G. W. Sutton and A. Sherman, "Engineering magnetohydrodynamics," McGraw-Hill, New York. USA, 1965.

[32] E. M. Abo-Eldahab and M. A. El-Aziz, "Hall and ion-slip effects on MHD free convective heat generating flow past a semi-infinite vertical flat plate," Phys. Scripta, vol. 61, p. 344, 2000.

[33] J. Buongiorno, "Convective transport in nanofluids applications of nanofluids: current and future," ASME J. Heat Trans., vol. 2010, pp. 240–250, 2006.